



Simulation of Particle Interactions with Matter in  
Soft Tissue, Water, and Bone Using PHITS  
Monte Carlo Code: Physical Aspects of Bragg  
Curve for Carbon Ion Therapy

---

Hassane El Bekkouri, El Mehdi Al Ibrahmi, Mohamed El-Asery,  
Adil Bardane, Zouhair Sadoune, Abdessamad Didi and  
El Mahjoub Chakir

EasyChair preprints are intended for rapid  
dissemination of research results and are  
integrated with the rest of EasyChair.

January 30, 2023

# Simulation of Particle Interactions with Matter in Soft Tissue, Water, and Bone Using PHITS Monte Carlo Code: Physical Aspects of Bragg Curve for Carbon Ion Therapy

Hassane El bekkouri  
*Dept. of Physics, Faculty of Science*  
*Ibn Tofail University*  
 Kenitra, Morocco  
 hassane.elbekkouri@uit.ac.ma

El mehdi Al ibrahmi  
*Dept. of Physics, Faculty of Science*  
*Ibn Tofail University*  
 Kenitra, Morocco  
 elmehdi.alibrahmi@uit.ac.ma

Mohamed El-asery  
*Dept. of Physics, Faculty of Science*  
*Ibn Tofail University*  
 Kenitra, Morocco  
 mohamed.el-asery@uit.ac.ma

Adil Bardane  
*Dept. of Physics, Faculty of Science*  
*Ibn Tofail University*  
 Kenitra, Morocco  
 adil.bardane@uit.ac.ma

Zouhair Sadoune  
*Dept. of Physics, Faculty of Science*  
*Ibn Tofail University*  
 Kenitra, Morocco  
 zouhair.sadoune@uit.ac.ma

Abdessamad Didi  
*National Energy Center of Nuclear Science and Technology*  
 Rabat, Morocco  
 a.didi@ump.ac.ma

El mahjoub Chakir  
*Dept. of Physics, Faculty of Science*  
*Ibn Tofail University*  
 Kenitra, Morocco  
 elmahjoub.chakir@uit.ac.ma

**Abstract**—Monte Carlo simulations are becoming widely regarded as the most accurate tool for calculating the interactions of particles with matter. In this study, we first investigated the influence of the average excitation energy of water ( $I_W$ ) on the Bragg Peak (BP) location. Second, we used the PHITS code to investigate the Bragg curve of  $^{12}C$  ion beams at energy of 200 MeV/u in three mediums: water, soft tissue, and bone. Third, we examine how secondary particles affect the overall dose. The results indicate that the position of the BP is strongly affected by the average excitation energy of water. The tail dose beyond the BP is generated mainly by secondary fragments of the primary carbon ion beams. In addition, PHITS has been shown to faithfully reproduce the measured Bragg curves.

**Index Terms**—Bragg peak, phits code, carbon ion therapy, simulation Monte Carlo

## I. INTRODUCTION

One of the most popular forms of treatment for malignant tumors is radiation therapy. Fast protons were first suggested for use in radiotherapy by Robert R. Wilson in 1946 [1] when he realized the potential of heavy charged particles. The therapeutic utilization of heavy ions, like carbon ion, has acquired great interest by reason of its physical and radiobiological benefits in comparison to X-ray therapy [2], [3]. The greatest advantage of these particles is their particular depth dose distribution, known as the Bragg curve, that is distinguished by a low dose at the entrance with a maximum dose deposition at the end of their range resulting in a dose

peak called the Bragg peak (BP) [4]. The charged particle has a larger ionization capacity and a higher linear energy transfer [5] in the BP region, which are related to an improved relative biological effectiveness (RBE) [6]. This Bragg curve is the result of a continuous interaction of charged particles with the atomic envelope of the target nuclei described by the Bethe-Bloch formula [7]:

$$-\frac{dE}{dx} = 2\pi r_e^2 N_a m_e c^2 \rho \frac{Z}{A} \frac{z^2}{\beta^2} \left[ \ln \left( \frac{2m_e v^2 \gamma^2 W_{max}}{I^2} \right) - 2\beta^2 - \delta - \frac{2C}{Z} \right] \quad (1)$$

Where:

$r_e$ : is the classical electron radius,  $N_a$ : Avogadro's number,  $m_e$ : mass of an electron,  $c$ : the speed of light,  $v$ : the particle velocity, with  $\beta = \frac{v}{c}$ ,  $\rho$ : the electron density of the medium traversed by the charged particle,  $Z$ : the atomic number of the medium absorbing,  $z$ : the charge of the projectile,  $\gamma = \frac{1}{\sqrt{1-\beta^2}}$ ,  $W_{max}$ : the maximum energy that can be transferred to an electron in a single collision,  $I$ : is the mean excitation energy of the absorbing medium in eV,  $\delta$  is the density correction to ionization energy loss in absorbing material and  $C$ : represent the shells correction to energy loss.

The mean excitation energy is of crucial importance because it determines the energy loss of the projectile and its range. For liquid water, The International Commission on Radiation

Units and Measurements (ICRU) report 37 recommends a value of  $I_w = 75$  eV [8]. Using the Monte Carlo simulation method with the Particle and Heavy-Ion Transport code System (PHITS) code [9], we analyze the impact of the average excitation energy of water ( $I_w$ ) on the position of the BP of the carbon-ion beams, and then examine the capabilities of the PHITS code to reconstruct experimental data published in the literature on the depth dose distribution in different media: water, soft tissue, and bone phantom.

## II. MATERIALS AND METHODS

Monte Carlo simulations are an efficient method for the numerical calculation of stochastic phenomena and have become an unavoidable tool for the study of radiation-matter interactions, also used in medical imaging [10]. It allows the provision of very precise information where experiments are either impossible or difficult to realize. Currently, the full Monte Carlo codes used for carbon ion therapy applications are established general-purpose codes such as Geant4 [11], FLUKA [12], [13] and PHITS [9], this last code that we used in this work.

PHITS is a general particle transport simulation code that can handle the transport of most types of particles with energies up to 1 TeV/u based on several nuclear reaction models and databases, developed by Japan Atomic Energy Agency (JAEA) and other institutes. This simulation code has been written in FORTRAN. It is based on an input file, in which are listed the parameters of the simulation, as well as the required observables. In the latest version (3.29) of PHITS, the Liège Intranuclear Cascade (INCL) model [14] is used to calculate the nuclear reactions induced by nucleons and light ions. The Kurotama model [15] was used for total nucleus-nucleus reaction cross section. The generalized evaporation model (GEM 2.0) [16] is used for the evaporation of light particles and the fission of excited residual nuclei. To evaluate the distribution of deposit energy below 20 MeV, the Event Generator Model (EGM) [17] has been integrated into the PHITS code. The Electron-Gamma Shower (EGS5) [18] algorithm was used to simulate the atomic interactions of electrons, positrons, and photons. To take into account the angular and energetic misalignment of the charged particles, two parameters ( $nedisp = 1$  and  $nspre = 2$ ) are used in the input file [19]. To calculate the energy losses of charged particles, PHITS uses the ATIMA [20] code with a continuous slowing down approximation.

In this study, we used a simple cylindrical phantom with a radius of 10 cm, bounded by two planes on the Z axis (0 and 40 cm) and located inside a central sphere of 500 cm radius. These dimensions were selected to match the dimensions of a representative tumor. Fig. 1 shows a carbon ion beam incident on a water phantom along the z-axis, the distance from the source being 20 cm in air. The primary number of carbon ions in this simulation was set to  $10^6$ . The Gaussian source with 0.5 cm full width at half maximum (FWHM) was taken into consideration in order to match the simulated geometry to the experimental study that was carried out at the GSI Darmstadt

facility of the biophysics group [24]. The relative error of all simulations in this study was less than 4%.

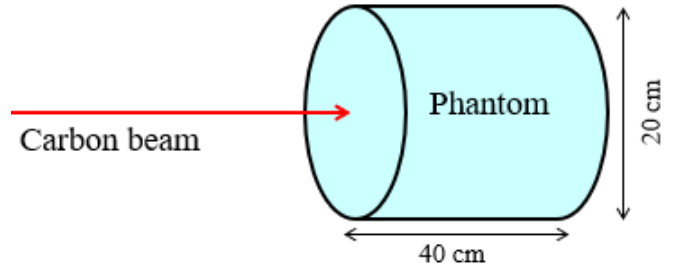


Fig. 1. A carbon ion beams hit a water phantom.

## III. RESULTS AND DISCUSSION

### A. Influence of the mean excitation energy of water ( $I_w$ ) on the Bragg curves position of $^{12}C$ ion beam

The mean excitation energy of water ( $I_w$ ) used in the Bethe-Bloch charged particle formula is recommended by ICRU reports (37,49,73,90). For liquid water, the measured energy loss for a 70 MeV proton is 79.7 eV [21], [22] and values of 75 - 78 eV from precise measurements of the Bragg curve for protons and various heavier ions [23]. The PHITS code uses the ATIMA code to calculate the stopping power of charged particles in water, and the ionization potential of water adjusted automatically to 75 eV (the value recommended by ICRU report 37 and 49). However, in the recent ICRU report 90 (2016), the mean excitation energy has been revised to a value of 78 eV. To investigate the influence of ( $I_w$ ) on BP position, we introduce, in input file, a parameter: ih2o and we calculate the depth-dose distribution with different ( $I_w$ ) values to investigate their influence on the BP position of  $^{12}C$  ion in water phantom. We simulate a beam with 200 MeV/u energy with different values of ( $I_w$ ). Fig. 2 and Table.1 demonstrate that PHITS faithfully reproduces the measured Bragg curves' form. The experimental data [25] is compared to the ranges of  $^{12}C$  predicted by PHITS at energy of 200 MeV/u. From this simulation, we see that the change in the value of ( $I_w$ ) leads to a spatial translation of the position of the Bragg peak: When we increase ( $I_w$ ) by 5 eV, the range increases by about 0.7 mm. According to the literature, for a given ionization model, the ( $I_w$ ) values must be known to within 5 eV for the accuracy on the range needed by hadron therapy to be 1 mm. The Bragg peak position and range, which are crucial elements in the treatment planning, are thus significantly influenced by the value of "ih2o" in the input file. However, It was more similar for both ( $I_w$ ) (75 eV, ICRU report 73) or (78 eV, ICRU report 90).

### B. Evaluation of the PHITS code for the Bragg curve of $^{12}C$ ion beams in water, soft tissue, and bone

In this study, we examined the BP location of  $^{12}C$  ion beams impinging on water, soft tissue, and bone. The density of water and soft tissue is  $1g/cm^3$  and that of bone is  $1.85g/cm^3$ . According to the ICRU standard, the bone is made

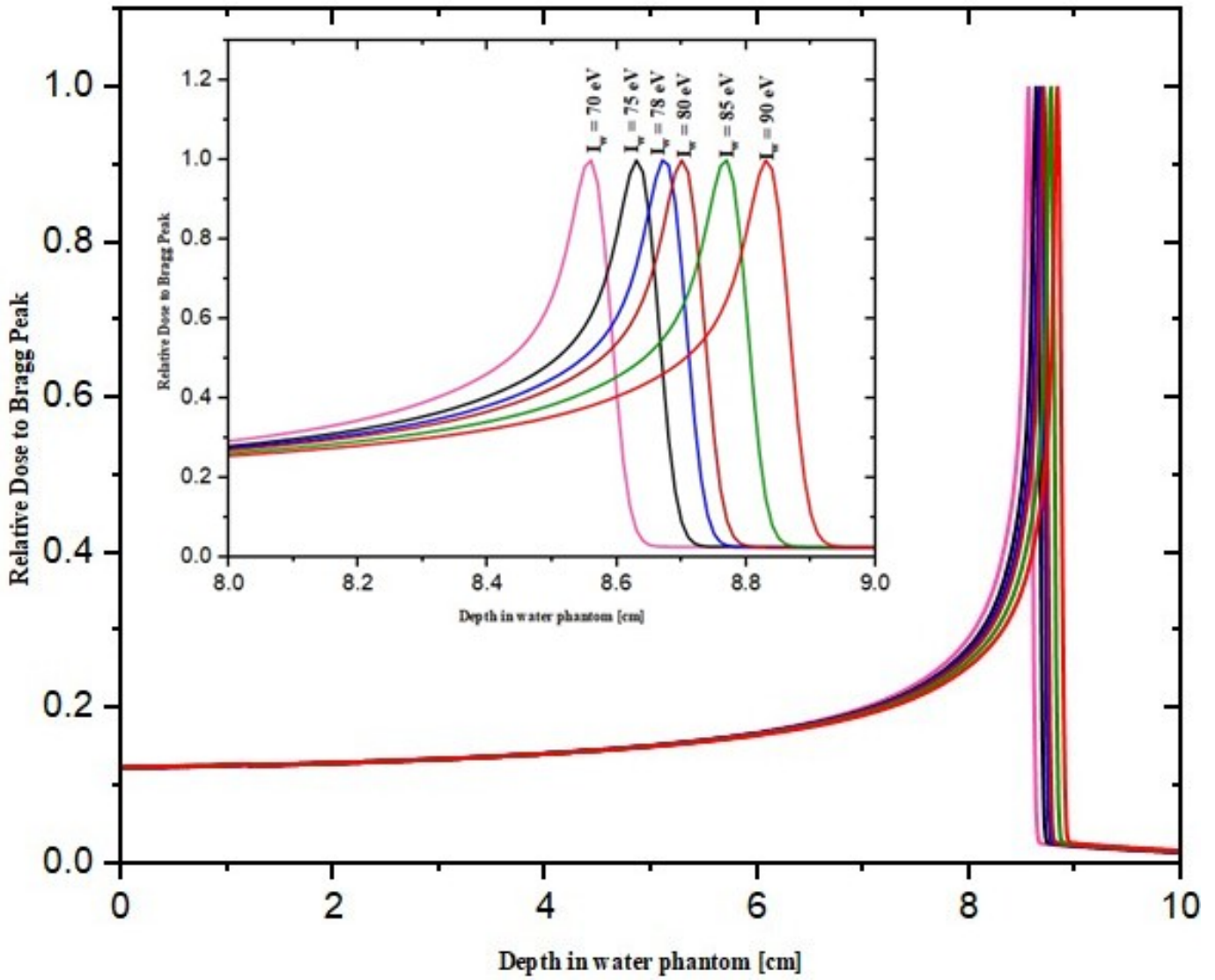


Fig. 2. Depth-dose distribution of  $^{12}\text{C}$  ion beams at energy of 200 MeV/u at different values of ( $I_W$ )

up of eight components: H(0.063984), C(0.278), N(0.027), O(0.410016), C(0.002), P(0.07), S(0.002), Ca(0.147) and for soft tissue: C(0.111), O(0.762), N(0.026) and H(0.1).

A comparison of the depth dose distributions in the three targets for a 200 MeV/u  $^{12}\text{C}$  ion beam is shown in Fig. 3 Both water and soft tissue exhibit the same dose drop characteristics, and both materials' PB are located quite close to one another. The BP was 4.97 cm in the bone, 8.67cm inside the water phantom, and 8.63 cm inside the tissue. Thus, in accordance with the literature [26], The peak sharpens in the medium with a higher electron density (bone medium) and is located at a shallower depth along the beam direction (Z-axis). The maximum energy deposited per source at 200 MeV/u in bone target was about  $6.2541 \times 10^{-8}$  Gy/source,  $6.6761 \times 10^{-8}$  Gy/source in soft tissue and  $6.6366 \times 10^{-8}$  Gy/source in water. Table. 2 shows the position of the Bragg peak in water, soft tissue, and bone for carbon ion beams of 200 MeV/u energy

and a comparison with other study using FLUKA code [27]. we conclude that PHITS code reproduces the results with high accuracy (does not exceed 5%).

### C. Secondary fragments' impact in the carbon ion beam's dose deposition in soft tissue

Nuclear fragmentation occurs in both the target and the projectile when a  $^{12}\text{C}$  ions beams traverses a medium. After the primary beam has entirely stopped, the fragmentation dose contribution clearly looks to be dominant beyond the peak point. There are more results on the fragmentation of  $^{12}\text{C}$  ion beams in the literature [28].

In this study we have using the PHITS code to investigate the contribution of primary and secondary beams to the total dose in water phantom. Fig. 4 shows the results of the simulation. As shown in this figure, the primary ion of  $^{12}\text{C}$  completely stopped at Bragg peak, while various secondary particles

TABLE I  
BRAGG PEAK POSITION OF  $^{12}\text{C}$  ION BEAMS AT 200MEV/U IN DIFFERENT MEDIUM

Energy beam(MeV/u)	Experimental range(cm)	Simulated range ( $I_w = 70eV$ )	Simulated range ( $I_w = 75eV$ )	Simulated range ( $I_w = 78eV$ )	Simulated range ( $I_w = 80eV$ )	Simulated range ( $I_w = 85eV$ )	Simulated range ( $I_w = 90eV$ )
200	$8.65 \pm 1mm$	8.56	8.63	8.67	8.70	8.77	8.84

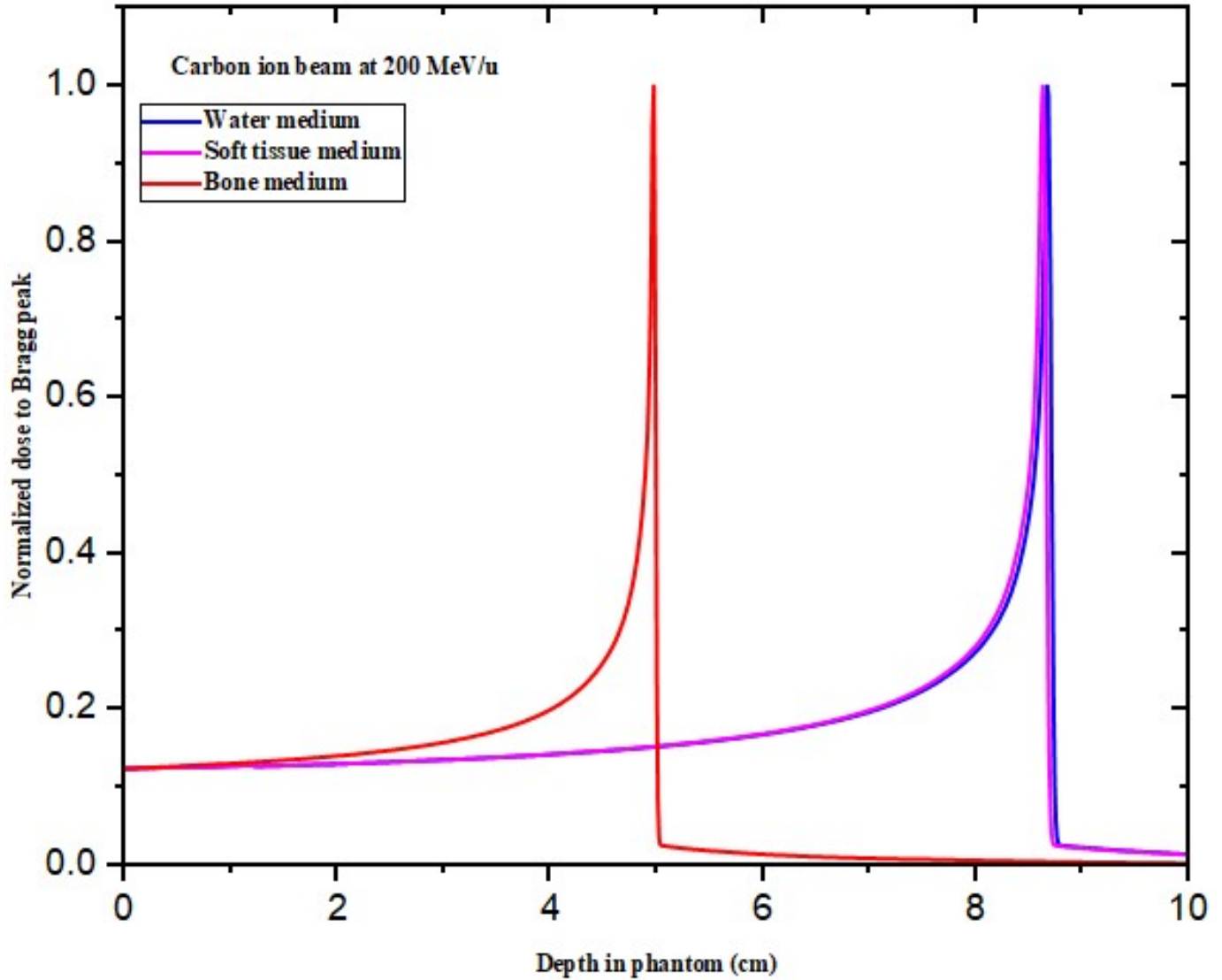


Fig. 3. Bragg peaks of  $^{12}\text{C}$  ion beams at 200 MeV/u in three medium

TABLE II  
DEPTH-DOSE OF  $^{12}\text{C}$  ION BEAMS AT ENERGY OF 200 MEV/U IN WATER, SOFT TISSUE AND BONE

Phantom target	Depth (cm) (this study using PHITS code)	Depth (cm) (Using FLUKA code)
Water	8.67	8.64
Soft tissue	8.63	8.68
Bone	4.97	4.93

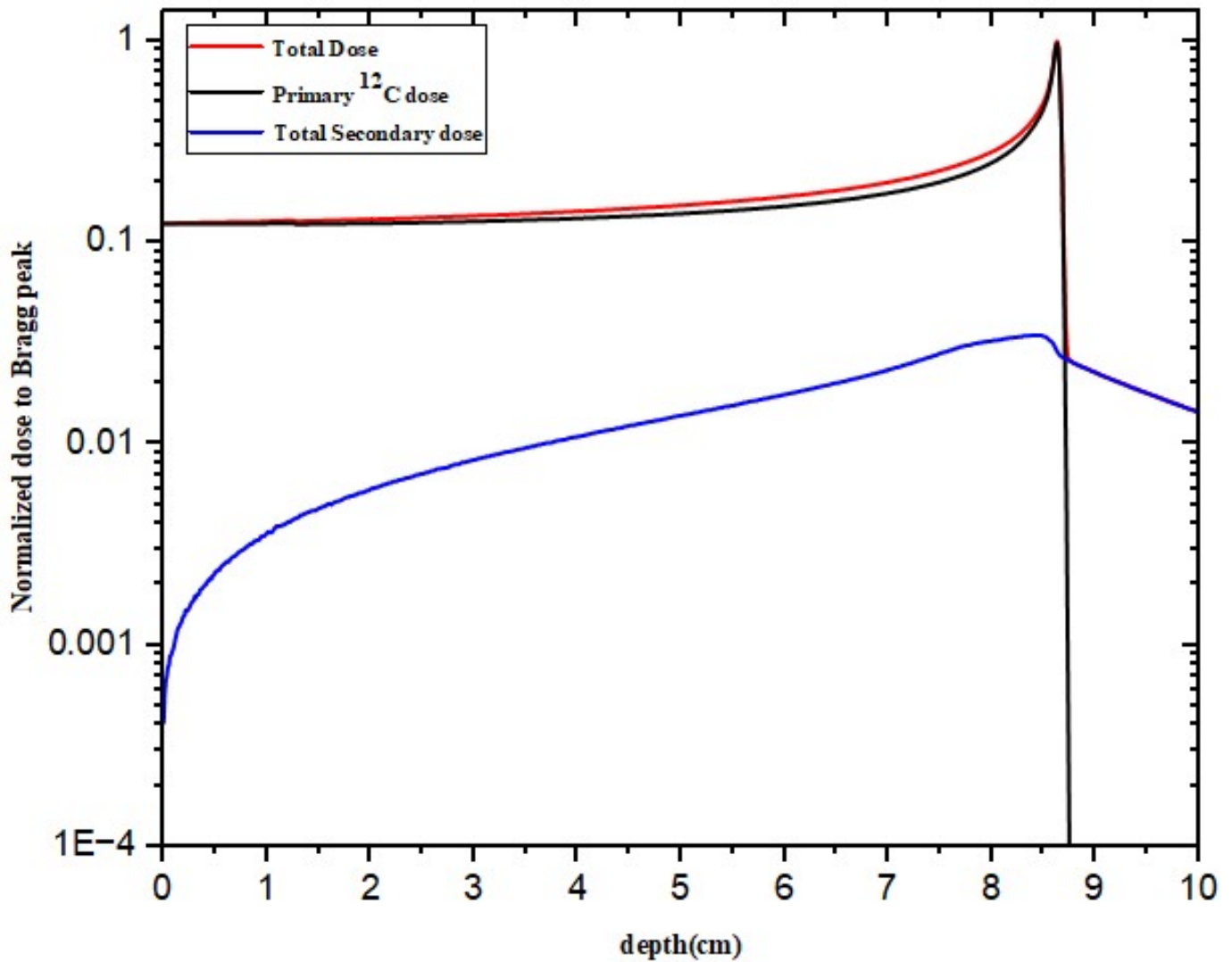


Fig. 4. Simulation using the PHITS code of Bragg curves for 200 MeV/u of  $^{12}\text{C}$  ion beams in water, with contributions from primary  $^{12}\text{C}$  ions and secondary fragments

create a tail deposited energy following the BP. Taking into account this dose will help with treatment planning. They make up roughly 10% of the entire dose.

To conclude, the BP placement into phantom is significantly impacted by the mean ionization energy of water (Fig. 2). In addition to the differing atomic numbers and densities of their respective compositions, the difference in ionization potential ( $I = 79.9$  eV for soft tissue and  $91.9$  eV for bone) is another factor contributing to the distinct beam behavior in bone and soft tissue (Fig. 3).

An advantage of  $^{12}\text{C}$  ion beam radiation is that it can deliver the maximal dose to the tumor with the least amount of harm to nearby healthy tissues. However, the distribution of dose may be affected by the energy deposited by secondary particles (Fig. 4).

#### IV. CONCLUSION

The PHITS Monte Carlo code was used to simulate three targets (water, soft tissue, and bone) exposed to a  $^{12}\text{C}$  ion beams with an energy of 200 MeV/u. The location of the Bragg peak was compared. In phantom, the bone displayed a substantially lower depth dose while receiving a higher radiation as a result of nuclear fragmentation.

To summarize, in this study, different physical characteristics of the  $^{12}\text{C}$  ions beam in bone, soft tissue, and water phantom were studied using Monte Carlo simulation with the PHITS code. The latter replicates the experimental depth-dose data in a medium with a precision of approximately 0.02cm.

#### ACKNOWLEDGMENT

The Particle and Heavy Ion Transport System (PHITS) code was made available to the authors by the Director of the Center for Computational Science & e-Systems at the

Japan Atomic Energy Agency (JAEA). We also acknowledge the contributions of the scientists from the Materials and Subatomic Physics Laboratory, faculty of science, Ibn Tofail University, Kenitra.

## REFERENCES

- [1] Wilson, R.R., Radiological Use of Fast Protons. *Radiology*, 1946. 47(5): p. 487-491.
- [2] Jäkel, O., Physical advantages of particles: protons and light ions. *Br J Radiol*, 2020. 93(1107): p. 20190428.
- [3] Saager, M., et al., Fractionated carbon ion irradiations of the rat spinal cord: comparison of the relative biological effectiveness with predictions of the local effect model. *Radiation Oncology*, 2020. 15(1): p. 6.
- [4] Amaldi, U. and G. Kraft, Radiotherapy with beams of carbon ions. *Reports on Progress in Physics*, 2005. 68(8): p. 1861.
- [5] Kantemiris, I., et al., Dose and dose averaged LET comparison of 1H, 4He, 6Li, 8Be, 10B, 12C, 14N, and 16O ion beams forming a spread-out Bragg peak. *Medical Physics*, 2011. 38(12): p. 6585-6591.
- [6] Karger, C.P. and P. Peschke, RBE and related modeling in carbon-ion therapy. *Phys Med Biol*, 2017. 63(1): p. 01tr02.
- [7] Pitarke, J.M., et al., The Z13 Correction to the Bethe-Bloch Energy Loss Formula. *Europhysics Letters*, 1993. 24(7): p. 613.
- [8] Berger M J, Inokuti M, Anderson H H, Bichsel H, DennisJA, Powers D, Seltzer S M and TurnerJ E 1984 Report 37: Stopping Powers for Electrons and Positrons. ICRU-37 (Bethesda, MD: International Commission on Radiation Units and Measurements)
- [9] Sato, T., et al., Features of Particle and Heavy Ion Transport code System (PHITS) version 3.02. *Journal of Nuclear Science and Technology*, 2018. 55(6): p. 684-690.
- [10] A. Bardane, J. Tajmouaati, and A. Maghnoouj, "Monte Carlo Simulation of a Special Phantom with Geant4 Application for Tomography," *Moscow University Physics Bulletin*, vol. 75, pp. 58-62, June 01, 2020 2020.
- [11] Agostinelli, S., et al., Geant4—a simulation toolkit. *Nuclear Instruments and Methods in Physics Research Section A: Accelerators, Spectrometers, Detectors and Associated Equipment*, 2003. 506(3): p. 250-303.
- [12] Ferrari, A and Sala, Paola R and Fassò, A and Ranft, Johannes, FLUKA: A multi-particle transport code (Program version 2005). CERN-2005-010, SLAC-R-773, INFN-TC-05-11, CERN-2005-10, 2005.
- [13] Battistoni G, C.F., Fasso A, Ferrari A, Muraro S, Ranft J, Roesler S, Sala PR. , The FLUKA code: description and benchmarking. 2007.
- [14] Boudard, A., et al., New potentialities of the Liège intranuclear cascade model for reactions induced by nucleons and light charged particles. *Physical Review C*, 2013. 87(1): p. 014606.
- [15] Iida, K., A. Kohama, and K. Oyamatsu, Formula for Proton–Nucleus Reaction Cross Section at Intermediate Energies and Its Application. *Journal of the Physical Society of Japan*, 2007. 76(4): p. 044201.
- [16] Furihata, S., The GEM Code - the Generalized Evaporation Model and the Fission Model, in *Advanced Monte Carlo for Radiation Physics*. 2001. p. 1045.
- [17] Koji Niita, Y.I., Tatsuhiko Sato, Hiroshi Iwase, Norihiro Matsuda, Yukio Sakamoto and Hiroshi Nakashima, A new treatment of radiation behaviour beyond one-body observables. *International Conference on Nuclear Data for Science and Technology*, (2007) 1167-1169, 2007.
- [18] Hirayama, H., et al., The EGS5 code system. 2005: Japan. p. 432.
- [19] Ounoughi, N., et al., Physical aspects of Bragg curve of therapeutic oxygen-ion beam: Monte Carlo simulation. *Polish Journal of Medical Physics and Engineering*, 2022. 28(3): p. 160-168.
- [20] Geissel H, S.C., Malzacher P, et al., ATIMA. Available from: <https://web-docs.gsi.de/weick/atima/>.
- [21] Bichsel, H. and T. Hiraoka, Energy loss of 70 MeV protons in elements. *Nuclear Instruments and Methods in Physics Research Section B: Beam Interactions with Materials and Atoms*, 1992. 66(3): p. 345-351.
- [22] Bichsel, H., T. Hiraoka, and K. Omata, Aspects of Fast-Ion Dosimetry. *Radiation Research*, 2000. 153(2): p. 208-219
- [23] H. Paul, "The mean ionization potential of water, and its connection to the range of energetic carbon ions in water," *Nuclear Instruments and Methods in Physics Research Section B: Beam Interactions with Materials and Atoms*, vol. 255, no. 2, pp. 435-437, 2007/02/01/ 2007.
- [24] Steidl, P., et al., Precision measurements of Bragg curves of light-ion beams in water. *Verhandlungen der Deutschen Physikalischen Gesellschaft*, 2008. 43(1): p. 1.
- [25] Haettner, E., et al., Experimental study of nuclear fragmentation of 200 and 400 MeV  $^{12}\text{C}$  ions in water for applications in particle therapy. *Physics in Medicine and Biology*, 2013. 58(23): p. 8265-8279.
- [26] Knoll, G.F., *Radiation detection and measurement*. 2010: John Wiley & Sons.
- [27] Soltani-Nabipour, J., et al., Evaluation of dose distribution from  $^{12}\text{C}$  ion in radiation therapy by FLUKA code. *Nuclear Engineering and Technology*, 2020. 52(10): p. 2410-2414.
- [28] Ying, C.K., et al., Contributions of secondary fragmentation by carbon ion beams in water phantom: Monte Carlo simulation. *Journal of Physics: Conference Series*, 2017. 851: p. 012033.